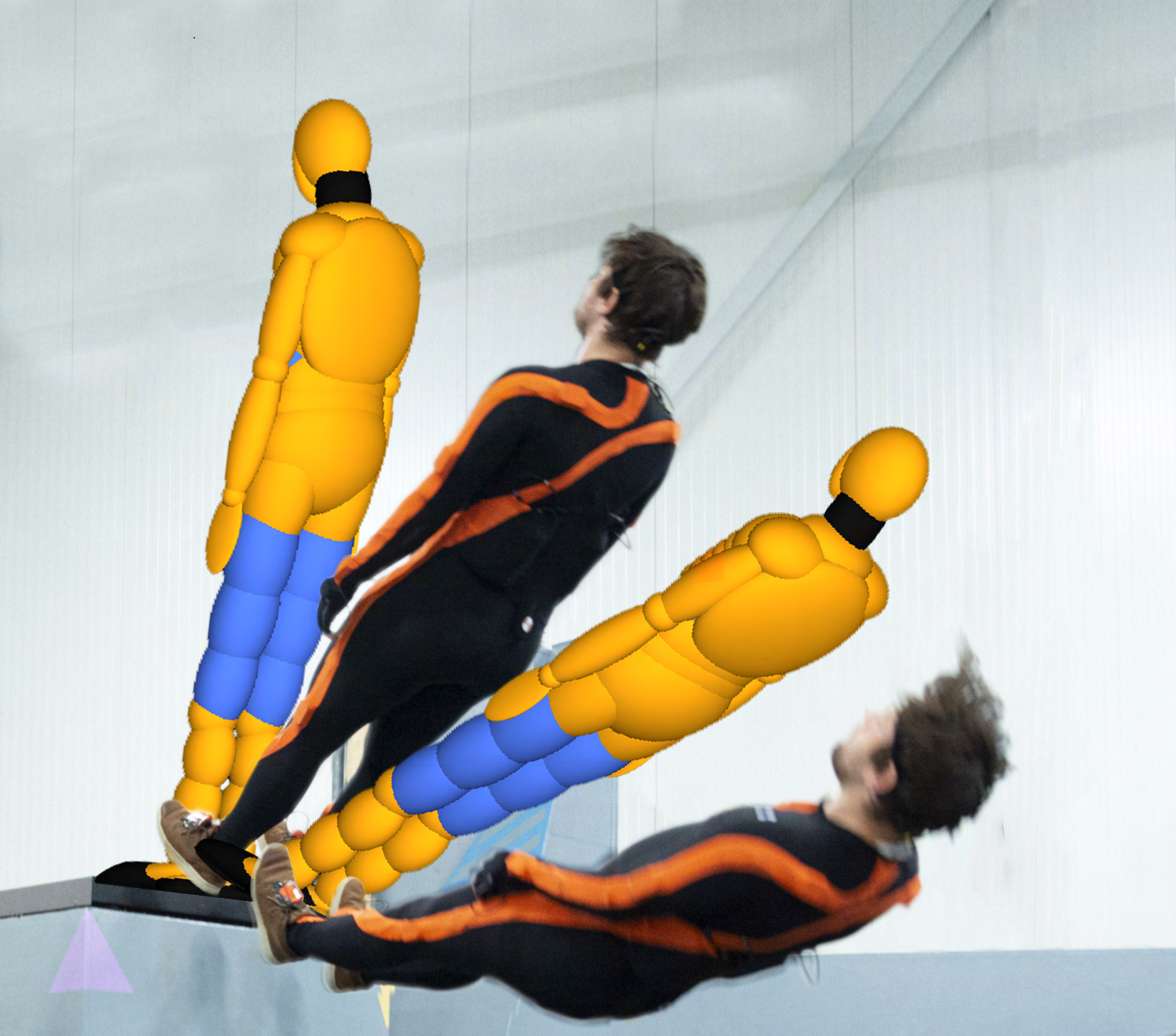

# Validation of Madymo Pedestrian Model for Reconstruction of Falling Incidents from Height

*Kim Hutchinson*

# Validation of Madymo Pedestrian Model for Reconstruction of Falling Incidents from Height

By

Kim Hutchinson
(Student number: 5155568)

in partial fulfilment of the requirements for the degree of

Master of Science
in Biomedical Engineering
Track I: Neuromusculoskeletal Biomechanics

at the Delft University of Technology,
Faculty of Mechanical, Maritime and Materials Engineering (3mE)

to be defended publicly on Monday July 4, 2022 at 13:30 PM.

| | | |
|---|---|---|
| Supervisors: | Dr. ir. A.J. Loeve, | TU Delft |
| | Dr. ir. W. Mugge, | TU Delft |
| | Dr. J.P. van Zandwijk | NFI |
| Thesis committee: | Dr. ir. A.J. Loeve, | TU Delft |
| | Dr. ir. W. Mugge, | TU Delft |
| | Dr. J.P. van Zandwijk | NFI |
| | Dr. ir. A. Seth | TU Delft |

TU Delft

Nederlands Forensisch Instituut
Ministerie van Justitie en Veiligheid

Forensic Engineering

carus

# Validation of Madymo Pedestrian Model for the Reconstruction of Falling Incidents from Height

K. Hutchinson

*Delft University of Technology, Mekelweg 5, 2628 CD Delft*

**Abstract**

Falls are a significant cause of injury-associated deaths. In cases where the events leading up to a fall are unclear, a forensic investigation may be required to uncover the cause. During the forensic reconstruction process, tools for objective scenario evaluation are needed. Computer simulations appear to be a promising tool for reconstructing falls, being cheaper in terms of both money and time than the alternative of physical scenario reconstruction. Although software packages intended for modelling the kinetics and kinematics of the human body exist, none were found that were validated specifically for fall reconstruction. The aim of the current study was to validate the performance of human body modelling software Madymo, intended for use in car-crash simulations, in reconstructing human falling movements. This was achieved by first performing experiments in which the kinematics and kinetics of participants were recorded during falls from a short height. Next, the initial conditions taken from the experimentally recorded falls were used as input to run corresponding simulations using Madymo. Finally, the results from the simulated falls were compared to those from the real falls, based on the posture just before landing. The results indicate that Madymo is currently not yet suited for use in reconstructing real human falls across multiple types of falls, and is therefore not yet fit for application in forensic investigations into falls.

## 1. Introduction

Falls are the second leading cause of injury-associated mortality.[1] The majority of falling incidents are handled by general or forensic practitioners, but some cases involving suspicious circumstances can give rise to questions regarding their cause, particularly in lethal cases. Distinguishing between an accident, suicide and violence is a difficult task that can require an extensive forensic investigation. The ultimate goal of such a forensic investigation is to reconstruct the events leading up to an incident, based on the known final state of a scene combined with other information, such as witness testimonies. During the process of a forensic reconstruction, there is a need for methods to evaluate scenarios. Unfortunately, efficient and validated objective scenario-evaluation methods for falling incidents are currently lacking and as a result, forensic investigations of this kind often produce dead-ends. One method that has been used is the physical reconstruction of scenarios using a dummy, though this is an expensive and time-consuming approach.[2,3] A cheaper alternative, in terms of both money and time, is to use numerical simulations with human body models to reconstruct and evaluate scenarios.

In order to reconstruct a scenario using numerical simulation, a set of initial conditions is defined for a model of the human body, and the kinematics and dynamics of the body are then computed forward in time based on physics. Although no commercial software has been developed for use in simulating human falling behaviour, commercial simulation software is available for application in car crash simulations. One software package that seems particularly suitable for application to the simulation and analysis of falls is Madymo. The Madymo human body models are extensively validated for application in car crash simulations, and as such it represents the kinematics of the human body well.[4]

Additionally, Madymo has built-in tools for predicting injury outcomes, such as skull fracture, which is promising for application to forensics. The human body models potentially suitable for fall-reconstruction in these car-crash simulation packages are the models used for simulating pedestrians, as the occupant models are constrained to initiate simulations in a car-seat. These pedestrian models are all passive models; no active movement is simulated. Of these pedestrian models, the Madymo 50$^{th}$ percentile pedestrian model is the most commonly used model for pedestrian impact reconstruction.[5]

There are several ways to use numerical simulations of an incident in the process of forensic reconstruction. One way is to use optimisation techniques to find one or multiple sets of initial conditions that will result in the body position, injury pattern and traces observed at the scene of a fall-incident. A drawback of this approach is that it provides no insight into the likelihood of a given scenario resulting in the observed outcome, compared to other scenarios in the case. Another approach is to perform a Monte Carlo simulation, in which a large number of falls is simulated, for a range of input conditions such as position and posture. The results from the Monte Carlo approach can then be used to make probability statements on the likelihood of the observed outcome occurring, for a range of initial conditions. Though more computationally intensive, the insight into the probability of fall-scenarios makes this a promising approach for application in a forensic context. The viability of this approach has been illustrated for use in forensic reconstructions of car-crashes by Moser & Spek.[6]

Several authors have used car-crash simulation software for the reconstruction of human falling-incidents for application in forensics. Adamec et al. have used the Madymo pedestrian model in forensic case reconstructions of falling incidents.[7] Muggenthaler et al., and Wach & Unarski did the same, using crash-simulation software PC-Crash instead of Madymo.[8,9] In Milanowiçz & Kędzior and Wiechel et al., Madymo simulations of fall-incidents are done using initial conditions based on experimental recordings of volunteers falling.[10,11] All three studies found a set of initial conditions that was able to explain the traces at the scene of the falling incident they were reconstructing. Han has used PC-Crash to execute a large number of fall-simulations with varying input conditions with the goal of applying the simulation results to the investigation of forensic fall-incidents.[12]

Currently, the main issue is that none of the commercially available human body models, including the ones in the Madymo family, have been validated specifically for application in fall-simulation. Quantifying the similarity between a modelled scenario and a case can only be done based on measures that can both be observed at the scene, and inferred from the model. In the case of fall-incidents, this may for example include final body position and injury patterns. As such, it is essential that those common measures are the same in a simulated and real incident, given the same initial conditions. Therefore, in order to apply numerical simulation to the forensic reconstruction of falls, it is crucial to first understand how well the given software performs in fall simulations specifically. The goal of the current study is to validate the use of the Madymo pedestrian model for the application of reconstructing human falling movements. This was achieved by first experimentally recording volunteers falling from a height, then using the initial conditions derived from those experiments to simulate those falls, and finally comparing the respective final states of the experimental falls to those of corresponding modelled falls. A schematic overview of the current study can be found in Appendix A.

## 2. Method

### 2.1. Experiment

During the experiment, kinematics and kinetics of participants falling from a height were recorded using inertial and visual motion capture systems, as well as force recording devices. Several types of falls were conducted, initiated through passively tilting over, pushing and jumping.

#### *2.1.1. Participants*

Nine healthy participants were recruited for the study: three female and six male. The mean (SD) age, height and weight of the participants were 26 (4) years, 181 (9) cm and 82 (15) kg, respectively. The experimental protocol was approved by the TU Delft Human Research Ethics Committee (submission number 1667). Before partaking in the experiment, participants provided informed written consent.

#### *2.1.2. Set-up*

The experiment was conducted in an exercise room equipped with a foampit (a large container filled with soft foam blocks) that participants could

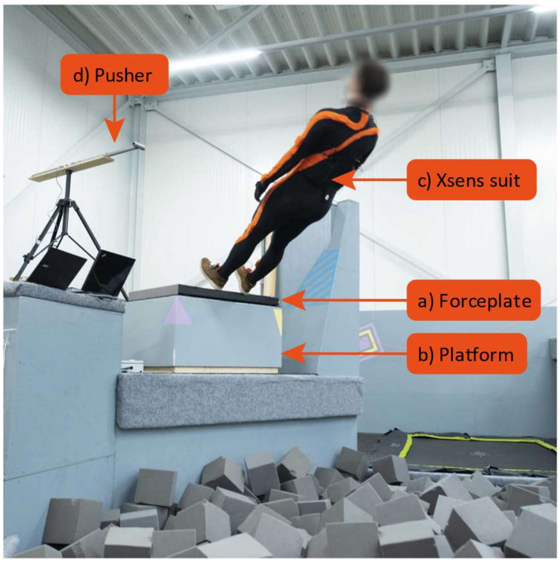


Figure 1 – A snapshot from one of the experimental trials. Pictured is a participant falling from the forceplate (a) on the platform (b) into the foampit. The participant is wearing an Xsens motion-capture suit (c). The device for pushing the participant into the pit can be seen on the left (d).

safely fall into from a low height (*Gymworld Zoetermeer, FreeRun Academy*).

A platform was positioned next to the pit, 1.5 meters above the edge of the pit (Figure 1). A forceplate (*ForceLink BV, Culemborg, The Netherlands*) was placed on top of the platform to record the vertical and fore-aft components of the ground reaction forces of the participant before falling into the foampit, as well as its point of application. Before the experiments, the forceplate was calibrated using a set of known weights (5 kg, 10 kg and 15 kg). The forceplate recorded data at a sample frequency of 1000 Hz.

The participant wore an Xsens motion capture suit (*MVN MT9, Xsens Technologies B.V., Enschede, The Netherlands*), which is a lycra suit embedded with a set of IMUs that record the kinematics of the wearer. After putting on the Xsens suit, each participant went through the calibration procedure described by the accompanying software (*MVN studio version 2.6.5., Xsens Technologies B.V., Enschede, The Netherlands*). The calibration procedure involved the participant taking several reference poses, such as a T-pose, and performing reference moves, such as a squat. MVN studio was used to record the kinematic data of the participant during the experiment, at a frequency of 120 Hz.

A markerless motion-capture system set-up developed by Geelen et al. was used to record the participants during the experiments.[13] This set-up used machine-learning techniques (*DeepLabCut*) to track features in video footage.[a] By recording footage from several angles simultaneously, the 2D trajectories of the tracked features could be combined to determine 3D-trajectories. A set of four cameras (*Raspberry Pi 4 Model B High Quality Camera Module KW-2906, with 6mm 3MP Lens KW-2908*) was used to record each trial from four different angles simultaneously, at a framerate of 40 Hz. The placement of the cameras around the foampit is shown in Figure 2. A set of five Raspberry Pi computers (*Raspberry Pi 4 Model B / 4GB KW-2504*) was used, one to operate each camera and one that controls the synchronisation by ensuring that each camera records each consecutive frame at exactly the same time as every other camera. Before the experiment, calibration recordings were done using a ChArUco calibration board, which is a checkerboard-like pattern printed onto large board.[b] These calibration recordings enable the integration of the simultaneously recorded 2D trajectories from the different cameras, into a single 3D trajectory.

During a subset of the trials, an external force was applied to push the subject into the foampit using a custom-made device, henceforth referred to as the 'pusher' (Figure 3). The pusher contained a uni-directional force sensor (*Keli Transducers Co. Model:PST, capacity 150 kg, 5C*), which recorded the magnitude of force used to push the participant. The pusher was constructed using light-weight materials such as pvc, so that inertia-effects resulting from the mass of the pusher itself were negligible with respect to the magnitude of the load applied to the participant. The pusher was mounted on a height-adjustable column tripod (*Manfrotto, 161MK2B*), level to the floor and perpendicular to the edge of the foampit. A schematic overview of the

Figure 2 – An overview shot of the foampit participants fell into. The orange circles indicate the four locations where the cameras of the PiCam systems were positioned during the experiment.

a http://www.mackenziemathislab.org/deeplabcut

b https://docs.opencv.org/4.x/da/d13/tutorial_aruco_calibration.html

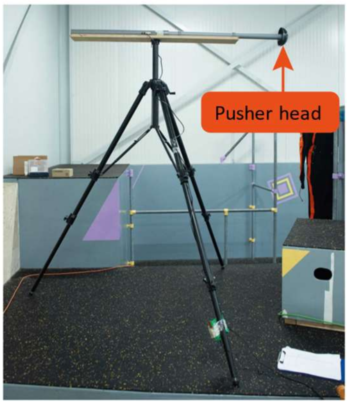


Figure 3 – The pusher, used to push participants into the pit during some of the experiment trials. The head of the pusher, which is the part that made contact with the participant, is on the right. The pusher is mounted on a height-adjustable column tripod.

complete experimental set-up can be found in appendix B.

### *2.1.3. Synchronisation*

Multiple computers were used simultaneously during the experiment to record the data, and the acquisition software packages for the devices were not integrated with each other. Therefore, to allow synchronisation of all the separate data streams described above, a synchronisation procedure was carried out before each trial. The participant stepped onto the forceplate, placing their feet at the marked locations (Figure 4), and briefly stood still. Next, the participant stamped down onto the plate with their left foot twice. The two force peaks recorded by the forceplate were synchronised with the kinematics recorded by the camera and Xsens systems. During the falls where the participant was pushed, the forceplate and pusher were synchronised before the subject stepped onto the forceplate. A wooden beam was placed on the forceplate, leaning against the pusher. The experimenter briefly pushed onto the beam twice, producing two peaks in the force signals of both the forceplate and pusher signals, which

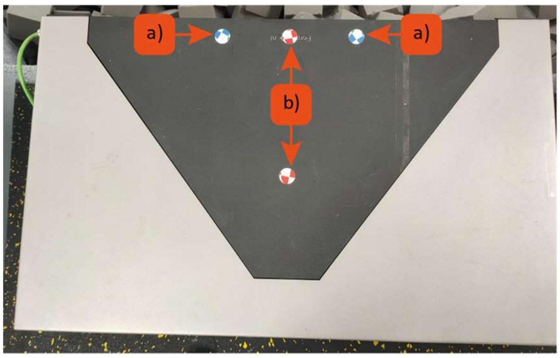


Figure 4 – Forceplate used to record participant's ground reaction forces. The circular red marks in the centre (a) indicate the locations for the participant's feet during sideways falls, the blue marks to the left and right (b) mark the foot positions during forward and backward falls.

were used to synchronise them. The synchronisation procedure is explained in-depth in Appendix C.

### *2.1.4. Experimental Protocol*

During each trial, the participant briefly stood still in upright position with their arms hanging by their sides, their feet placed at the marked locations on the forceplate (Figure 4), before falling into the foampit. The falls were initiated under six different sets of initial conditions, divided into three categories:

- **Passive**: The participants were instructed to slowly lean into the direction of the pit and allow themselves to tilt over and fall, while remaining as passive as possible. No falls in forward direction were conducted, since this would have put the participants at risk of back-injury.
  - Backwards fall *(PaBa)*: Participant stood with their back towards the fall-direction.
  - Sideways fall *(PaSi):* Participant stood with their left side towards the fall-direction.
- **Pushed:** The pusher was placed in contact with the participant The experimenter manually applied a push-force to the participant using the pusher, until the participant fell. As such, the peak push force was not identical each time but ranged from 69 to 152 N. The participant was warned before they were pushed.
  - Backward *(PuBa)*: Participants stood with their backs towards the fall-direction. The pusher-height was adjusted such that the push-force was applied at the sternum.
  - Sideways *(PuSi)*: Participants stood with their left sides towards the fall-direction. The pusher-height was adjusted such that the push-force was applied to the upper arm, approximately 10 cm below shoulder height.
- **Active:**
  - Jumped forward *(JuFo)*: Participants were facing the fall-direction. They were instructed to jump forward, aiming for the centre of the pit, which was about 1.5 meters from the edge of the platform.
  - Stepped forward *(StFo)*: Participants stood facing the fall-direction. They were instructed to step off the edge of the platform, by placing a foot forward off the edge of the platform and

without generating more forward momentum than needed to clear the edge of the pit.

Figure 5 shows snapshots of typical trials for each of these falling conditions. Each of the six falling conditions was consecutively repeated three times, so each participant performed a total of 24 falls into the foampit. However, due to technical issues with data-acquisition resulting in missing camera footage, participants number 2 and 8 were excluded from further analysis. An additional nine trials were excluded from the analysis due to data-acquisition issues resulting in missing data, leaving a total of seven participants and 159 valid trials.

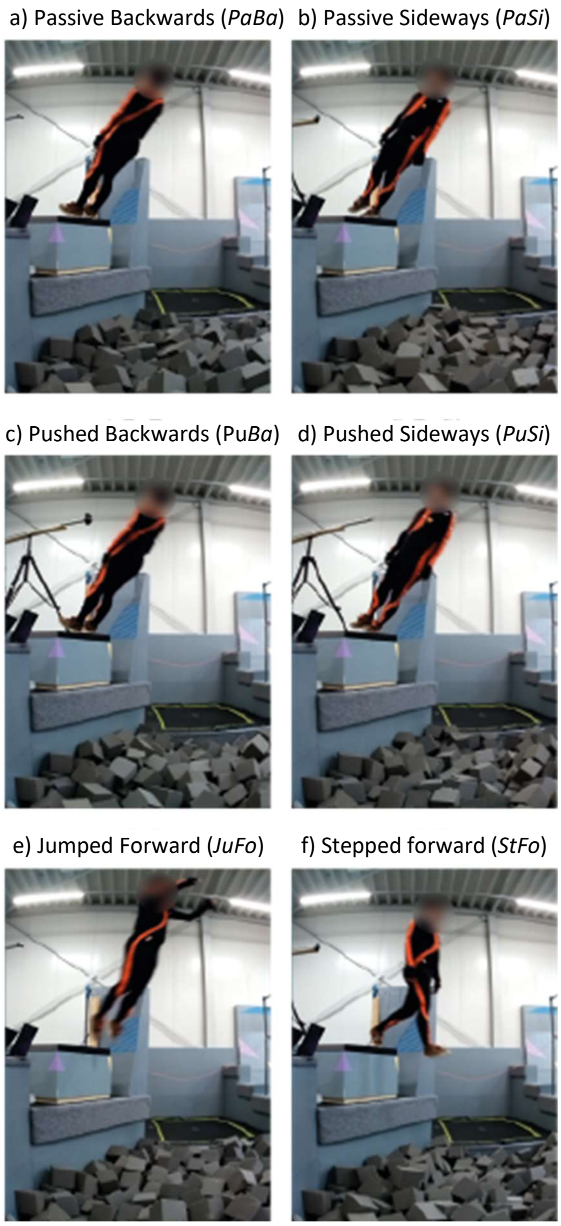


Figure 5 – Snapshot of typical trials for each of the falling conditions, a) passive backwards, b) passive sideways, c) pushed backwards, d) pushed sideways, e) jumped forward, f) stepped forward.

The order of the fall-types for each of the participants was assigned using a balanced Latin square for participants 2-8, and randomised for participants 9 and 10. Participant number 1 was part of a pilot recording and is not included anywhere. The **active** falls were recorded for potential future use, and were not included in the simulations or result analysis. See Appendix D. for an overview of the order of the falls for each participant.

## 2.2. Modelling

### *2.2.1. Madymo*

Forward-dynamic simulations were executed for every valid trial from the **passive** and **pushed** experiments using car-crash reconstruction software Simcenter Madymo$^{TM}$ (*Siemens Industry Software and Services BV*). A Madymo scene was built consisting of a platform for the human model to fall from, and a floor 2 m below the platform (Figure 6). The platform was set to output the ground reaction force of the human model on the platform. The human body model used was a scalable Madymo human pedestrian model (*version 5.2, 'h_ped50el_inc.xml'*). A scaled model was created for each participant using Madymo's built-in *Dummy/Human model scaling tool*, based on each participant's respective gender, weight and height. The model was initialised on top of the platform, with its feet 1 cm above the platform to ensure no penetration of the feet into the platform would occur in the initial state.

### *2.2.2. Initial Conditions and Modelling Choices*

As the goal of the current study was to determine whether the Madymo pedestrian model is able to reproduce the kinematics of the experimentally recorded falls, a trial-and-error method was adopted to select initial conditions and modelling settings that resulted in falling movements that resembled the experimental falls.

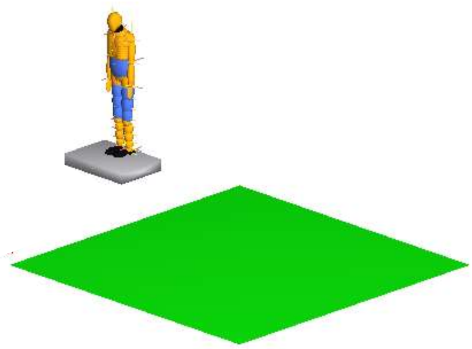

Figure 6 – The scene used for the Madymo simulations. The model is standing on top of the platform from which the falls are initiated.

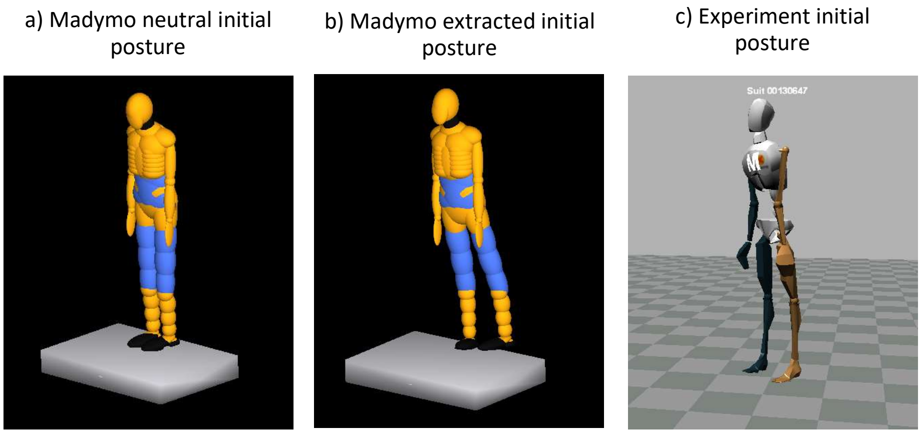


Figure 7 – An example of: a) a neutral Madymo initial position, b) a Madymo initial position as converted from an experimental trial, and c) the corresponding actual initial posture as seen in the Xsens software.

The considerations for the four main factors making up the initial conditions and settings for the simulations are as follows:

- **Initial Posture:** The initial posture of the model during the simulations was implemented in two ways, producing two sets of simulation setups. In one set, the initial posture of participants was taken from the experiment and used as the initial position for the dummy during the corresponding simulation. However, it was found that in a number of trials, when the posture of the participant, as obtained from the kinematics produced by the Xsens suit, was applied to the Madymo pedestrian model, it resulted in joint range of motion limits of the model being exceeded, likely due to a combination of calibration errors and drift in the Xsens kinematics. In addition, even given an identical combination of joint angles, the model posture did not always look exactly the same as the Xsens posture, as the definitions of their respective joints' degrees of freedom did not match exactly for every joint. Therefore, a second set of simulations was conducted with the neutral position as it is defined in Madymo, rather than the posture extracted from the experiment. Figure 7 shows the Madymo model in the neutral posture, as well as in a posture extracted from a typical experimental trial with the corresponding screenshot of the Xsens posture.

  The Xsens software denoted the participant kinematics for each body-segment in the form of segment origin coordinates along with 3D orientation quaternions. The Madymo pedestrian model accepted quaternions as input for a subset of joint types, but required Euler angles for others. For the joints that required Euler angles as input, the Xsens quaternions were converted to Euler angles first, before being used as input for the model. Additionally, not all the local coordinate systems of the body segments coincided between the Xsens output and Madymo model. In these cases, additional angle conversions were performed. An overview of the applied joint orientation input types can be found in Appendix E.
- **Initial Velocity:** In the case of the **passive** falls, an initial velocity had to be included, since there were no external forces initiating the falling movement. In the experiment, the velocity of the participant depended on which phase of falling over they were in. Therefore, in order to determine the initial velocity to be used for the model simulations, the experimental velocity of the participant was determined at four time instances (referred to henceforth as *T1, T2, T3* and *T4*) during the fall. These time instances were equally spaced in time between the last time instance the participants stood still before the fall, and the time instance the participant dropped off the platform and the ground reaction force returned to zero. The linear and angular velocities of the pelvis-segment of the participant were determined at these time instances, and applied at the model's *h-point*, which is a joint that connects the model to the environment and allows the user to input the orientation and velocity of the whole human model. Simulations were executed using these four velocities and the corresponding postures at time instances *T1, T2, T3* and *T4*.

  For the **pushed** falls, no initial velocity was included in the simulation, as the movement of the model was generated by the push-force. During these experiments, the participant stood still before they were pushed, so their initial velocity was zero.
- **Locking of Joints:** For both the **passive** and **pushed** falls, the knee and hip joints were locked in their neutral extended positions

during the full simulation. This was done because the model is passive, if these joints were left unlocked the model immediately collapsed, not even falling towards the pit.

- **External Force:** An external push force was applied only for the simulations of the **pushed** falls. The force signal of the complete push was extracted from the pusher output and applied at the centre of mass of the torso or shoulder of the model, for backwards and sideways falls respectively.

An overview of all the simulation setups that were executed, and the terms used to refer to them, can be found in Figure 8.

## 2.3. Analysis

### *2.3.1. Outcome Measures*

To compare the simulation results to the experiment, a set of three outcome measures was defined (Figure 9):

- **Whole-body rotation:** The participant's local axis of rotation was defined as a vector pointing from their pelvis to their head. The whole-body rotation is defined in degrees as the rotation of the participant around this local axis at the end-time, with respect to initial position of a backwards fall. As such, during the sideways falls, the fall is initiated with 90° whole-body rotation.
- **Ledge angle:** The ledge angle is defined in degrees as the angle between the participant's local-axis at the end-time, and the horizontal edge of the platform they are falling off of. The ledge angle is then corrected by -90 degrees, so that falling perfectly perpendicular to the edge results in a ledge angle of 0 degrees.
- **Vertical angle:** The vertical angle is defined in degrees as the angle between the participant's local axis at the end-time, and the global vertical axis.

These outcome measures were determined for each trial, for both the experimental and the modelled falls. In order to insightfully compare them between experiment and model, the two needed to be synchronised. In general, the length of time between the start of an experimental fall and the time instance the participant dropped off the forceplate was found to be shorter than the time between the start of a simulation and the time instance the model dropped off the platform. Therefore, in order to compare the model and experiment during a comparable phase of the fall, the outcomes were synchronised based on the time i nstances the participant/model dropped off the forceplate/platform and the vertical component of the ground reaction force became zero. The end-time at which the outcome measures were determined was then set at 0.3 seconds after drop-off for both experiment and model, as this was found to be the time instance just before participants hit the foampit.

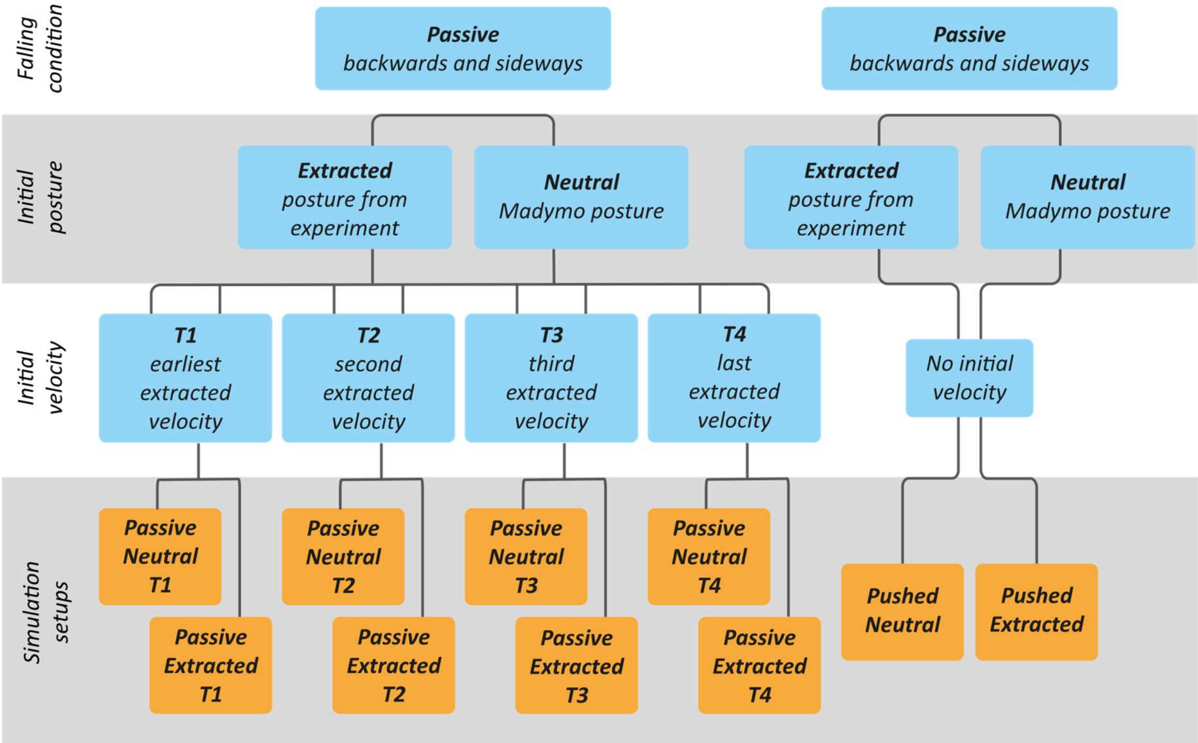


Figure 8 – An overview of the different setups used for the simulations. The top three rows each represent an aspect of a simulation setup: from top to bottom: falling condition, initial posture and initial velocity. Each block indicates which variants of that aspect were implemented in a simulation setup. The blocks in the bottom row each represent one simulation setup that was implemented.

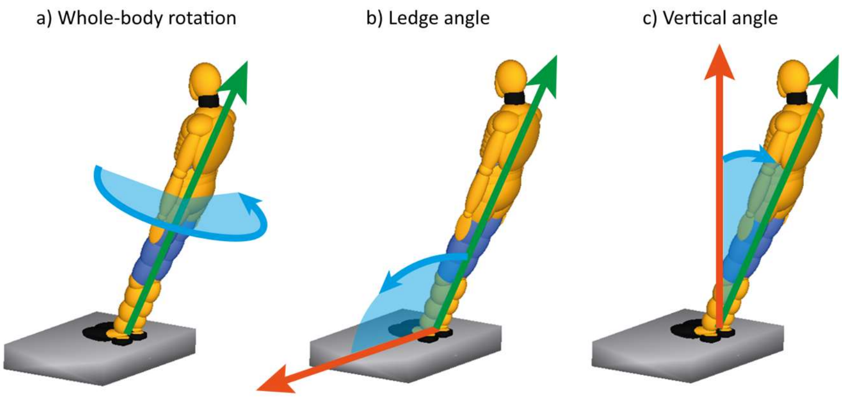

Figure 9 – The three outcome measures based on which the experiment and simulations were compared, illustrated using a Madymo model: a) whole-body rotation, b) ledge angle and c) vertical angle.

### *2.3.2. Statistics*

To determine whether the different falling conditions within the experiment resulted in outcomes that differed significantly from one another, the **passive** and **pushed** as well as the **backwards** and **sideways** falls were compared on all three outcome measures. Normality of the differences between conditions for all three outcome measures was rejected based on K-S tests, thus a non-parametric test was required to compare the conditions. Due to the repeated measures design, the same participants performed falls for all conditions, Wilcoxon signed-rank tests were used to compare the conditions.

Wilcoxon signed-rank tests were also conducted within each of the simulation setup, to determine if the outcomes significantly differed between conditions within each simulation setup. If the falling conditions within the experiment could be distinguished based on the outcomes, it was expected that if the model functions well, the conditions could also be distinguished within the simulation outcomes, and vice versa.

The performance of the model was assessed by comparing the outcomes of the experiment to the outcomes of each of the simulation setups. Here too, normality of the differences between the model and experiment for all three outcome measures was rejected based on K-S tests. Wilcoxon signed-rank tests were conducted to determine if significant differences existed between each of the simulation setups and the experiment.

The agreement per outcome measure between the results from the simulations and the experiment, was evaluated for each simulation setup using a set of Bland-Altman plots. Each point in the plots represents a single participant for a backwards or sideways falling condition. The mean of each participant's outcome value from the experiment with the corresponding outcome value from the simulation, was plotted against the difference between those outcomes. The difference was computed by subtracting the simulation outcome value from the experiment outcome value. The mean of all the differences, as well as the limits of agreement (mean ± 1.96 SD) are also indicated in the Bland-Altman plots.

Finally, for each simulation setup, the outcome values from all modelled participants were averaged, once for the backwards falling condition and once for the sideways falling condition. The experiment outcome values from all participants were also averaged, for the backwards and for the sideways falls. For each falling condition, the averaged values of the outcomes from the simulation setups were plotted against the differences between the averages of the simulation setups and the averages from the experiment, computed by subtracting the simulation averages from the experiment averages. Each point in the plots indicates a single simulation setup.

### *2.3.3. Synchronisation*

In order to insightfully compare the outcome measures between experiment and model, the two needed to be synchronised. The length of time between the start of an experimental fall and the time instance the participant dropped off the forceplate was found to be shorter than the time between the start of a simulation and the time instance the model dropped off the platform. Therefore, in order to compare the simulation and experiment during a comparable phase of the fall, the outcomes were synchronised based on the time instances the participant and model dropped off the forceplate and platform respectively, and the vertical component of the ground reaction force became zero. The end-time was then set at 0.3 seconds after drop-off for all results, which was found to be the time instance just before participants hit the foampit.

# 3. Results

The complete set of experimental data, simulations, and code is under embargo at the time of writing, but will become available on the 4TU.ResearchData repository.[14]

## 3.1. Experiment

Figure 10 provides an overview of the whole-body rotation, vertical angle and ledge angle, grouped by falling condition. While comparing the falling conditions, a significant difference was found in the whole-body rotation between the **backwards** (MD=10.0°, SD=11°) and **sideways** (MD=87.4°, SD=34°) falls, Z=3.3, p=.001. Note that **sideways** falls were initiated at a whole-body rotation of 90°, while **backwards** falls were initiated at 0°. A significant difference was also found in the ledge angle between the **backwards** (MD=3.7°, SD=6°) and **sideways** (MD=-8.9°, SD=12°) falls, Z=-2.9, p=.004. This means when falling backwards, participants tended to fall more towards their left, while sideways falls tended more towards the right of the platform. No significant difference in vertical angle was found between **backwards** and **sideways** falls.

The whole-body rotation also differed significantly between the **passive** (MD=28.1°, SD=36°) and the **pushed** (MD=45.4°, SD=54°) falls, Z=2.0, p=.048. No significant differences were found in the ledge angle or vertical angle between **passive** and **pushed** falls. The complete results of the statistical test are reported in Appendix F.

## 3.2. Modelling

Figure 11 shows synchronised snapshots from the Xsens and camera footage, along with a corresponding Madymo simulation from a typical **pushed** trial, at three time instances, starting from the moment the push force is applied to the participant. The whole-body rotation, ledge angle and vertical angle for each simulation set-up and each fall-direction were grouped by **backwards** or **sideways** falling condition and plotted in Figure 12.

Tests were conducted for every simulation set-up to compare the **backwards** and **sideways** falling conditions for each of the outcomes and the full test-results are reported in Appendix F. Statistically significant differences were found in the whole-body rotation between the **backwards** and **sideways** falls for all passive simulation setups, except *Passive Extracted T3,* and not for the pushed simulation setupus. Overall, where the difference was significant the whole-body rotation was positive and higher for **sideways** falls than for **backwards** falls, except for *Passive Neutral T4*, where the **backwards** falls resulted in higher whole-body rotations than the **sideways** falls. Again, note that **sideways** falls were initiated at a whole-body rotation of 90°, while **backwards** falls were initiated at 0°.

Differences were also found between **backwards** and **sideways** falls in the ledge angle for all simulation setups except *Passive Extracted T3.* Where the difference was significant the mean ledge angle was lower and negative for **sideways** than for **backwards** falls for all setups except for *Passive Extracted T3*, where it was the other way around.

The vertical angle was found to differ significantly between the **backwards** and **sideways** falls for *Pushed Extracted; Passive Neutral T1, T2 and T3; and Passive extracted T4.* The mean vertical angles, for both **backwards** and **sideways** falls was over 90° for all simulation setups, which means the model fell into a head-down position, with its pelvis being higher than its hips. For all setups where the difference in ledge angle between the **backwards** and **sideways** falls was significant, the **backwards** falls resulted in higher vertical angles than the **sideways** falls.

## 3.3. Comparison

Figure 13 contains the Bland-Altman plots showing the level of agreement between the experiment and each simulation setup per outcome measure. Tests were conducted to compare the outcomes of each simulation setup to the corresponding experimental outcomes. The complete results of the tests are reported in Appendix F.

For the whole-body rotation, significant differences between the experiment and simulation were found only for the *Pushed Neutral, Passive Neutral T1, Passive Neutral T2 and Passive Neutral T4* setups, with respective average values higher than the whole-body rotations found in the experiment. The difference in ledge angle between experiment and model was found to be significant for all simulation setups except for *Passive Extracted T4* and *Extracted Pushed*. Where the differences in ledge angle were significant, the average ledge angles per simulation setup were lower by 0.8° to 17.9° than those in the experiment, except for *Passive Neutral T4,* where it was 20.3°

higher. Finally, for the vertical angle the difference between model and experiment was significant for every single simulation setup. The vertical angle for model simulation setups was on average 66.4° to 89.5° higher than those found in the experiment

The agreement of all simulation setups with the experiment is summarised per backwards and sideways falling condition for each outcome measure in Figure 14. It can be seen in this figure that the simulation setup with the least difference with the experiment is a different one for each outcome measure and falling condition.

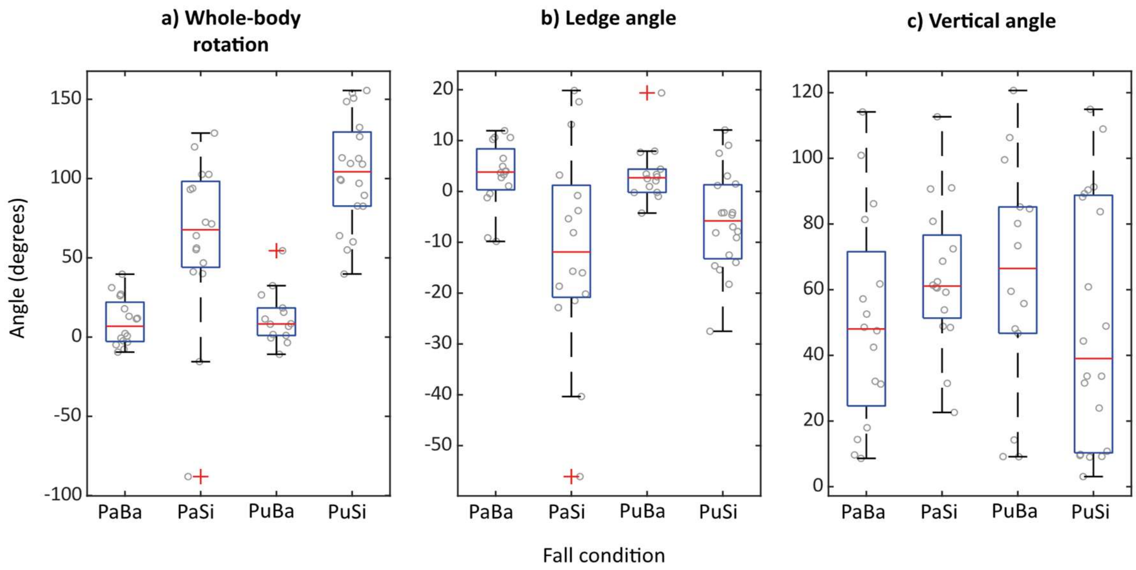


Figure 10 – The three outcome measures in degrees, whole-body rotation (a), ledge angle (b) and vertical angle (c), grouped per fall condition, passive backwards (*PaBa*), passive sideways (*PaSi*), pushed backwards (*PuBa*) and pushed sideways (*PuSi*).

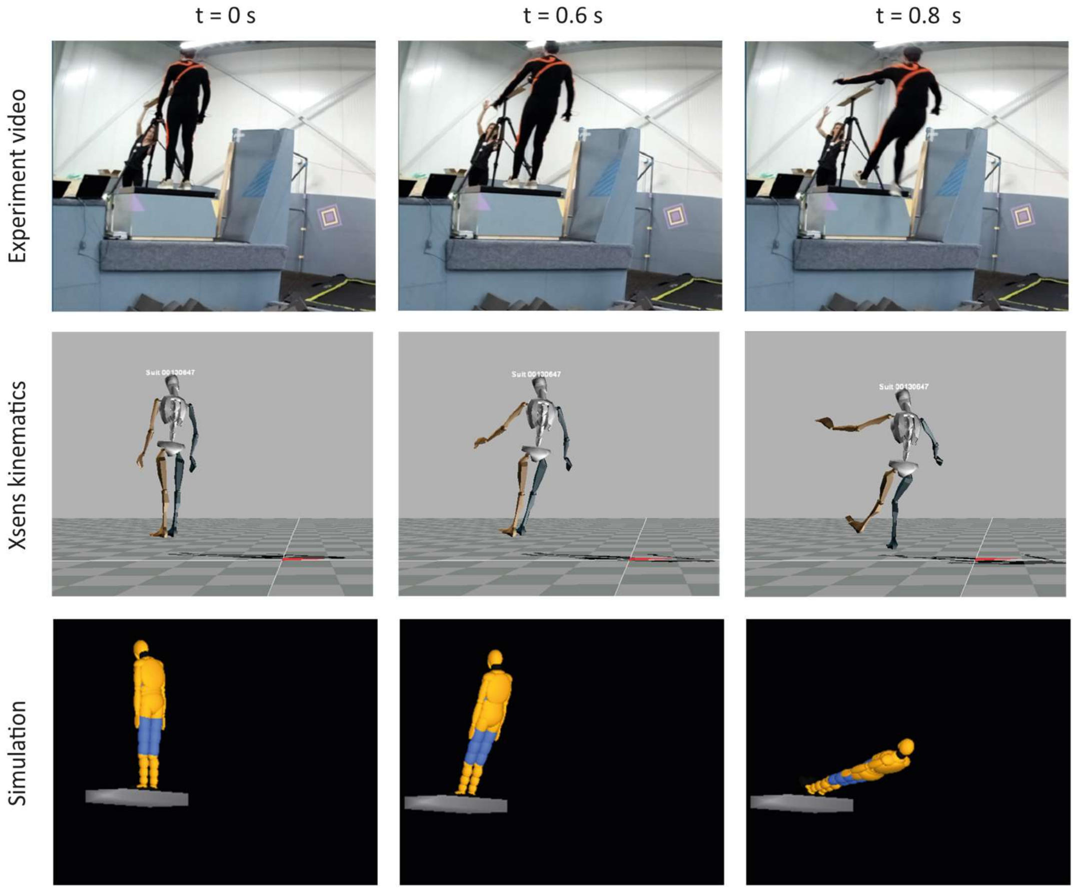


Figure 11 – Snapshots from a typical pushed fall experiment camera (top) and Xsens (middle) footage and a corresponding Madymo simulation (bottom), at the three time instances noted at the top of the figure: t=0 s, t=0.6 s and t=0.8 s, where t=0 s corresponds to the moment a push force is applied.

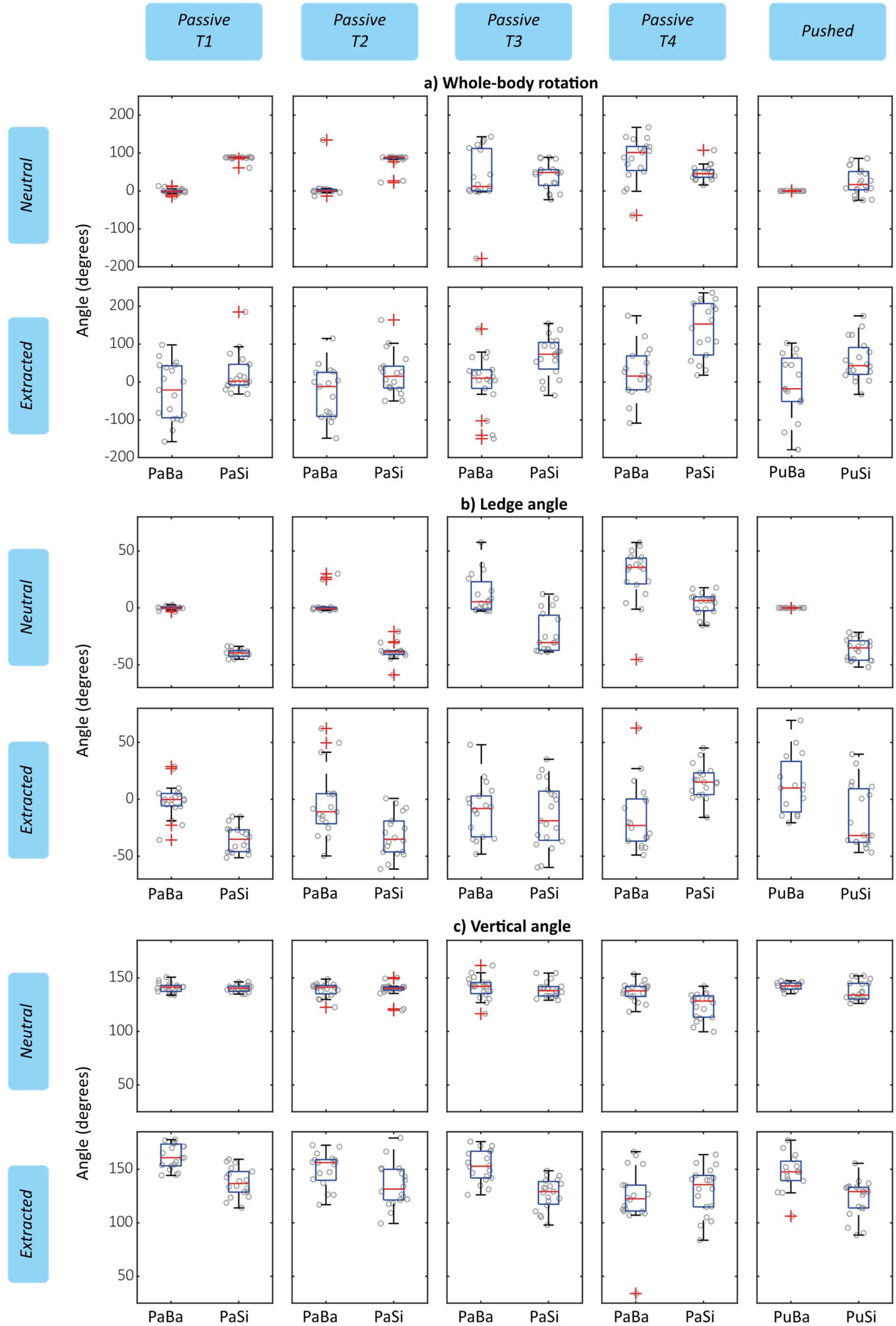


Figure 12 – The outcome measures: a) whole-body rotation, b) ledge angle and c) vertical angle for each of the simulation setups, grouped by falling condition. The text boxes at the top and left indicate which simulation setup is plotted in each column and row. The descriptions of the simulation setups can be found in Figure 8.

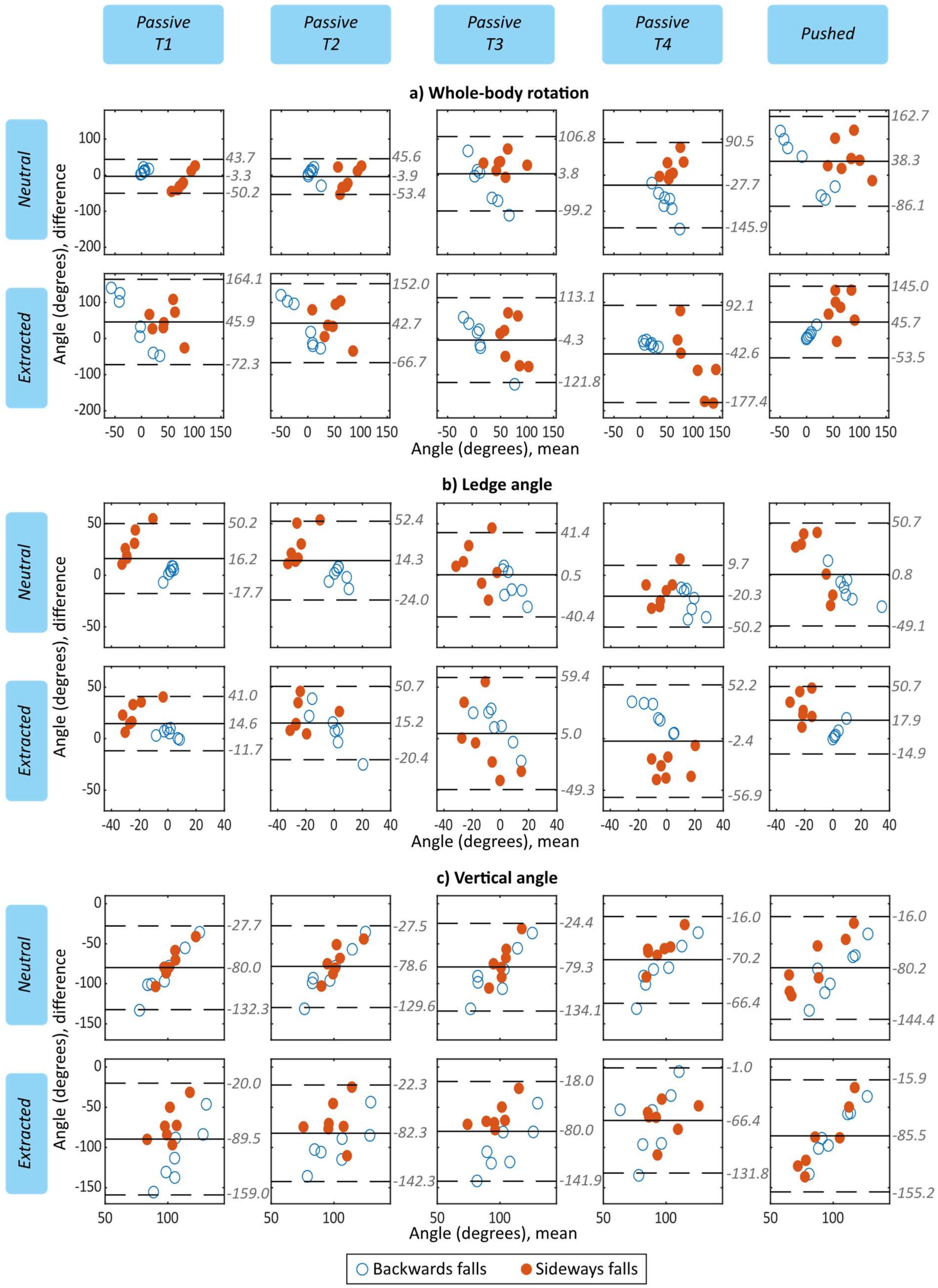


Figure 13 – Bland-Altman plots showing the level of agreement between the experiment and each simulation setup (explained in Figure 8), for a) the whole-body rotation, b) ledge angle and c) vertical angle. The mean of the simulation setup outcome with the experiment is plotted against the difference between them, determined by subtracting the simulation outcomes from the experiment outcomes. This is explained in-depth in section 2.3.2. A solid line was plotted to indicate the mean value of the difference, and the dashed lines represent the 95% limits of agreement (±1.96 SD), the values of the mean and limits of agreement are noted to the right of each plot.

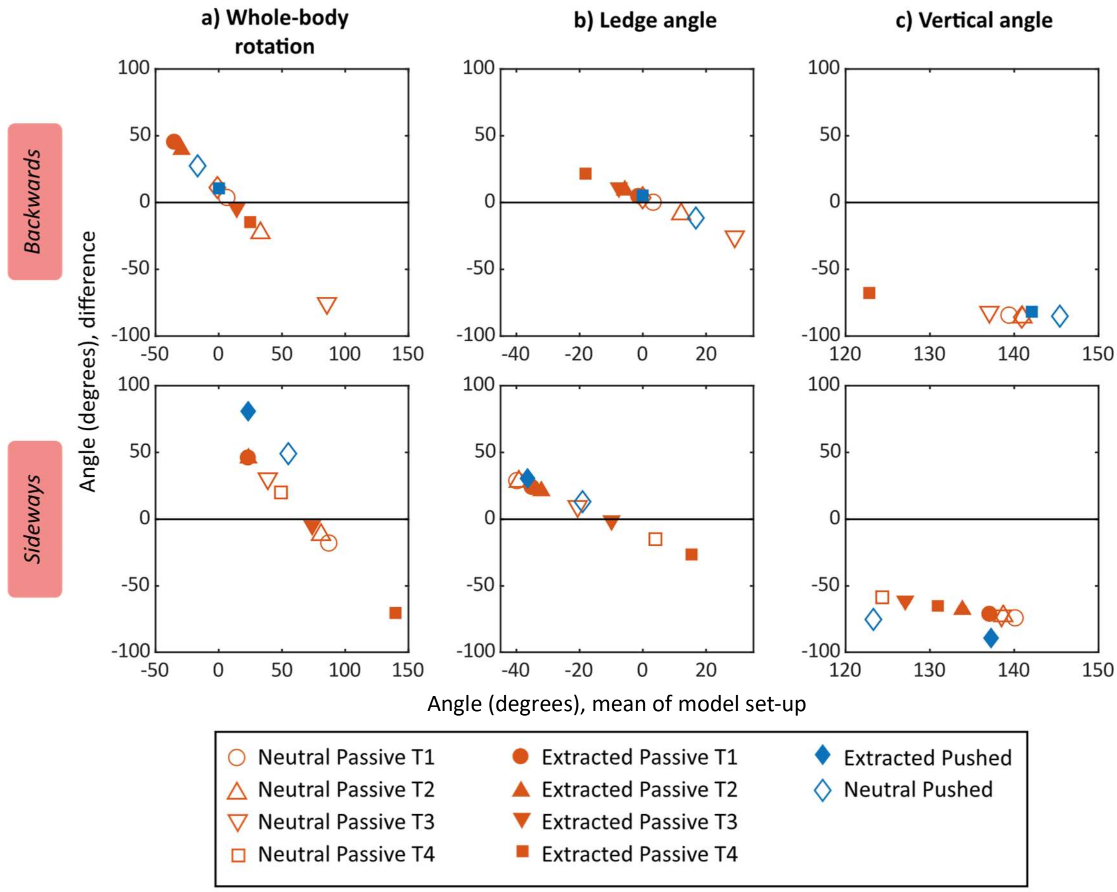


Figure 14 – Overview of the level of agreement of all simulation setups (see Figure 8) with the experiment for a) the whole-body rotation, b) the ledge angle and c) the vertical angle. The mean of all outcomes was determined per simulation setup and plotted against the difference with the corresponding mean from the experiment, determined by subtracting the model value from the experiment value. This is explained in-depth in section 2.3.2.

## 4. Discussion

The results suggest that the Madymo pedestrian model does not consistently reproduce the experimentally recorded falling movements across multiple falling conditions and outcome measures. A number of different setups were implemented to conduct simulations of the experimentally recorded falls, varying in how the initial posture and initial velocity were implemented. While several of the simulation setups used produced outcome values that were close to those in the experiment, this held only for specific conditions, subjects or outcomes. No 'best' set-up could be determined: for each of the conditions, a different setup was determined to produce outcome values closest to the experimental outcomes. It became clear during the modelling process that a lengthy process of case-by-case trial-and-error in selecting the precise model set-up could be used to produce results more accurately matching the experiment for a specific context, but this would make it impossible to generally apply the model when the either the outcome or the initial conditions of the fall being reconstructed are not known, such as would be the case in forensic applications.

The performance of the Madymo ellipsoid pedestrian model in reproducing human falling movements depended on the type of fall, as well as on the chosen setup for the simulation. The differences between model and simulation were most prominent in the vertical angle. All simulation setups produced average vertical angles between 66° to 90° higher than those found in the experiment. As the model tilted over, falling off the ledge, it kept its rotational movement during the entire fall. In the experiment, many participants were observed to perform corrective movements that prevented them from rotating to vertical angles much higher than 90°, likely in an attempt to prevent them from landing on their heads. Since the model is completely passive, it makes sense that the results of the corrective movements made by humans are not accurately reproduced in the model and the model does tend to end up with its head down.

It was expected that the outcomes of the **passive** and **pushed** falls in the experiment would differ significantly from each other. However, it was found that only the whole-body rotation differed between these conditions, not the ledge angle or vertical angle. This leads us to one of the limitations of the experimental set-up used to collect data: the falling movements exhibited by participants during the experiment may not fully represent actual dangerous or lethal falls, as participants were aware that the fall was safe and they knew when it was coming. It is possible that this is part of the reason why no significant difference was found between the **passive** and **pushed** falls, as we expect that a pushed fall in a real situation would provoke a much stronger corrective response than was observed in the current experiments. Future studies of falling behaviour may be improved by performing falling experiments in which participants are not made aware when and if they will fall. Like was done in a study of human response to falls by Milanowicz and Kedzior, where participants unexpectedly fell a brief height using VR immersion.[10]

The falling movements that were recorded in the current study were initiated under a limited number of simple circumstances. Even if the model performed well at reproducing the falling conditions recorded in the current study, further validation would be required of more varied cases, for example where a subject trips, falls over a railing or falls from initial positions other than standing upright. An additional forensically relevant outcome measure of the falls that should be assessed in future research is the horizontally travelled distance from the edge. Unfortunately, in the current study this could not be reliably extracted due to significant drift in the global position reported in the Xsens kinematic data.

As it was shown that the Madymo model did not consistently and accurately reproduce either the **passive** or the **pushed** falls experimentally recorded in the current study, steps should be taken in the future to improve the model. A first step would be to perform a sensitivity analysis on the effects of the various input conditions on the outcome measures, to figure out the best avenue to improving the model. For example, incorporating active balance control into the model may prevent the dummy from falling over in unexpected directions due to very small imbalances in initial postures, as is observed in the current model.

# 5. Conclusion

The Madymo pedestrian model currently did not consistently reproduce human falling movements across different falling conditions and subjects. Some simulation setups were created that produced outcomes that were close to the experimental values for specific participants or conditions, but as none did so consistently, this would require case-by-case tweaking when applied to the reconstruction of real falls. As such, the model in its current form is not yet suited to the reconstruction of falls for forensic purposes and needs to be improved, for example by implementing some form of active movement.


# Acknowledgements

I would like to express my gratitude to my supervisors Jan Peter van Zandwijk, Winfred Mugge and Arjo Loeve, from whom I have learned more than I could have imaged, both on the technical as well as the mental aspects of writing a thesis.

I would also like to thank Koen Wösten for the never-ending technical and emotional support. A big thanks to my housemates for always listening to both my rambling excitement and my extensive complaints, as well as for distracting me when I needed it most.

Finally, I am incredibly grateful to my parents, without whose loving support and unquestionable faith in me I would never have made it far enough to work on this fantastic project.

## References


1. Greenwood R, Hopkins A. Muscle responses during sudden falls in man. *The Journal of Physiology*. 1976;254(2):507-518. doi:10.1113/jphysiol.1976.sp011242
2. van Ee C, Raymond D, Thibault K, Hardy W, Plunkett J. Child atd reconstruction of a fatal pediatric fall. *ASME International Mechanical Engineering Congress and Exposition, Proceedings*. 2010;2:395-400. doi:10.1115/IMECE2009-12994
3. Schulz BW, Lee WE, Lloyd JD. Estimation, simulation, and experimentation of a fall from bed. *Journal of Rehabilitation Research and Development*. 2008;45(8):1227-1236. doi:10.1682/JRRD.2007.06.0092
4. Madymo S. Simcenter Madymo Human Body Models Manual October 2020. 2020;(October).
5. Shang S, Masson C, Llari M, et al. The predictive capacity of the MADYMO ellipsoid pedestrian model for pedestrian ground contact kinematics and injury evaluation. *Accident Analysis and Prevention*. 2021;149. doi:10.1016/J.AAP.2020.105803
6. Moser M, Steffan S, Spek S, Makkinga M. Application of the monte carlo methods for stability analysis within the accident reconstruction software PC-CRASH. *SAE Technical Papers*. 2003;2003(724). doi:10.4271/2003-01-0488
7. Adamec J, Graw M, Praxl N. Numerical simulation in biomechanics - a forensic example. *Acta Gymnica*. 2006;36(4):33-38.
8. Muggenthaler H, Drobnik S, Hubig M, Schönpflug M, Mall G. Fall from a balcony-accidental or homicidal? Reconstruction by numerical simulation. *Journal of Forensic Sciences*. 2013;58(4):1061-1064. doi:10.1111/1556-4029.12148
9. Muggenthaler H, Hubig M, Meierhofer A, Mall G. Slip and tilt: modeling falls over railings. *International Journal of Legal Medicine*. Published online 2020. doi:10.1007/s00414-020-02432-8
10. Milanowicz M, Kędzior K. Active numerical model of human body for reconstruction of falls from height. *Forensic Science International*. 2017;270:223-231. doi:10.1016/j.forsciint.2016.10.009
11. Wiechel J, Freyder D, Metzler S, Kloppenborg N. HUMAN FALL EVALUATION USING MOTION CAPTURE AND HUMAN MODELING. *Proceedings of the 14 th International Mechanical Engineering and Exposition*. Published online 2013:1-8.
12. Han I. Characteristic analysis and fuzzy simulation of falls-from-height mechanics, and case studies. *Forensic Science International*. 2020;311. doi:10.1016/j.forsciint.2020.110287
13. Geelen JE, Branco MP, Ramsey NF, van der Helm FCT, Mugge W, Schouten AC. MarkerLess Motion Capture: ML-MoCap, a low-cost modular multi-camera setup. *Proceedings of the Annual International Conference of the IEEE Engineering in Medicine and Biology Society, EMBS*. Published online 2021:4859-4862. doi:10.1109/EMBC46164.2021.9629749
14. Hutchinson K, Van Zandwijk JP, Mugge W, Loeve AJ, (2022): ICARUS: Modelling Human Falls for Forensics - Passive Models. *4TU.ResearchData. Dataset.* https://doi.org/10.4121/20054996

## Appendix A. Study Overview

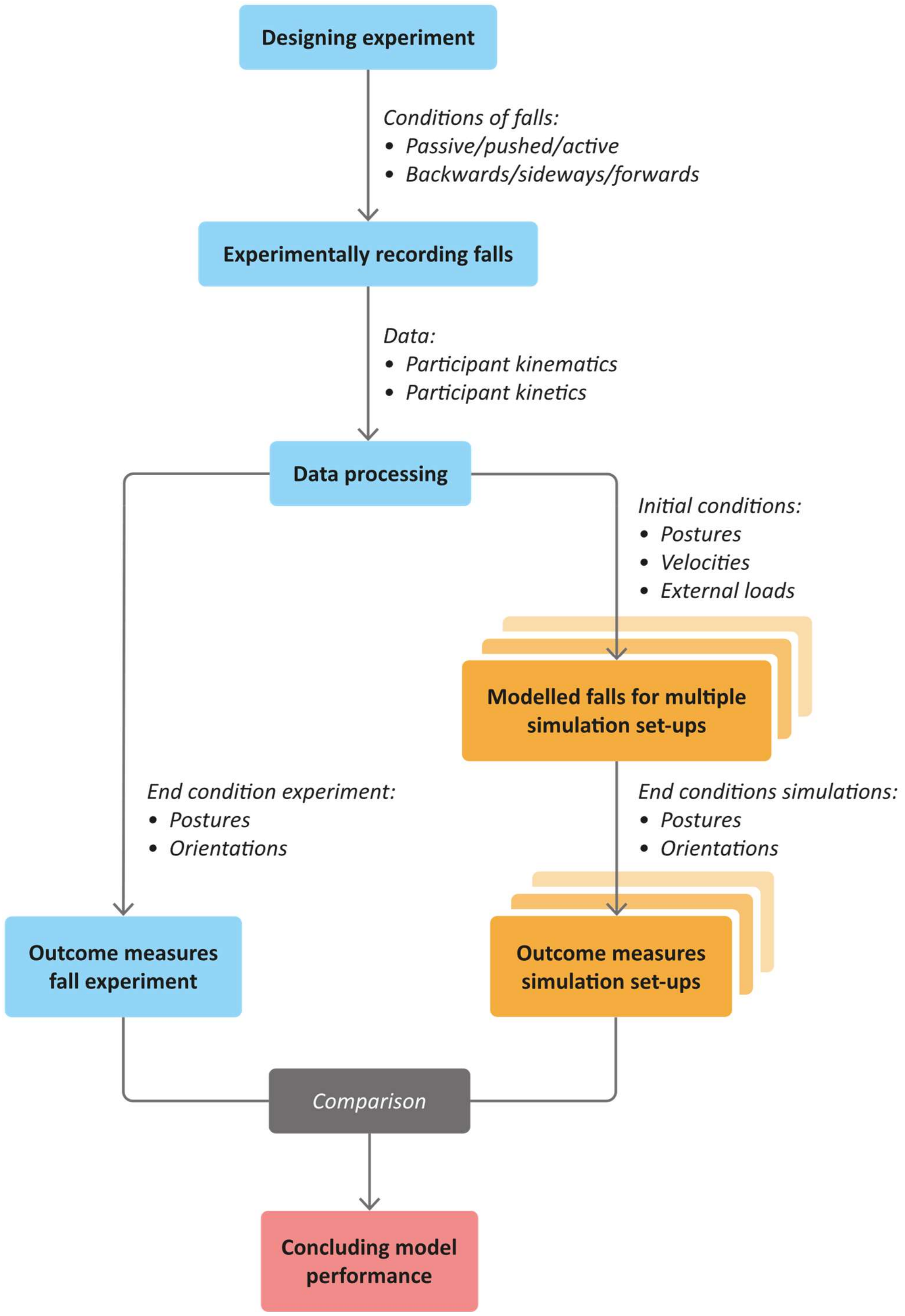


Figure 15 – An overview of the steps involved in the current study, starting from top to bottom. An experiment was designed in which participants fell a from a short height, with different conditions initiating the falls. The kinetics and kinematics of participants were recorded during these falls. The initial postures, velocities and external loads were used to run corresponding simulations, using several different setups. The outcomes from these simulated falls were compared to the outcome measures from the experimental falls, which was used to judge the performance of the model.

## Appendix B. Schematic Overview Experiment

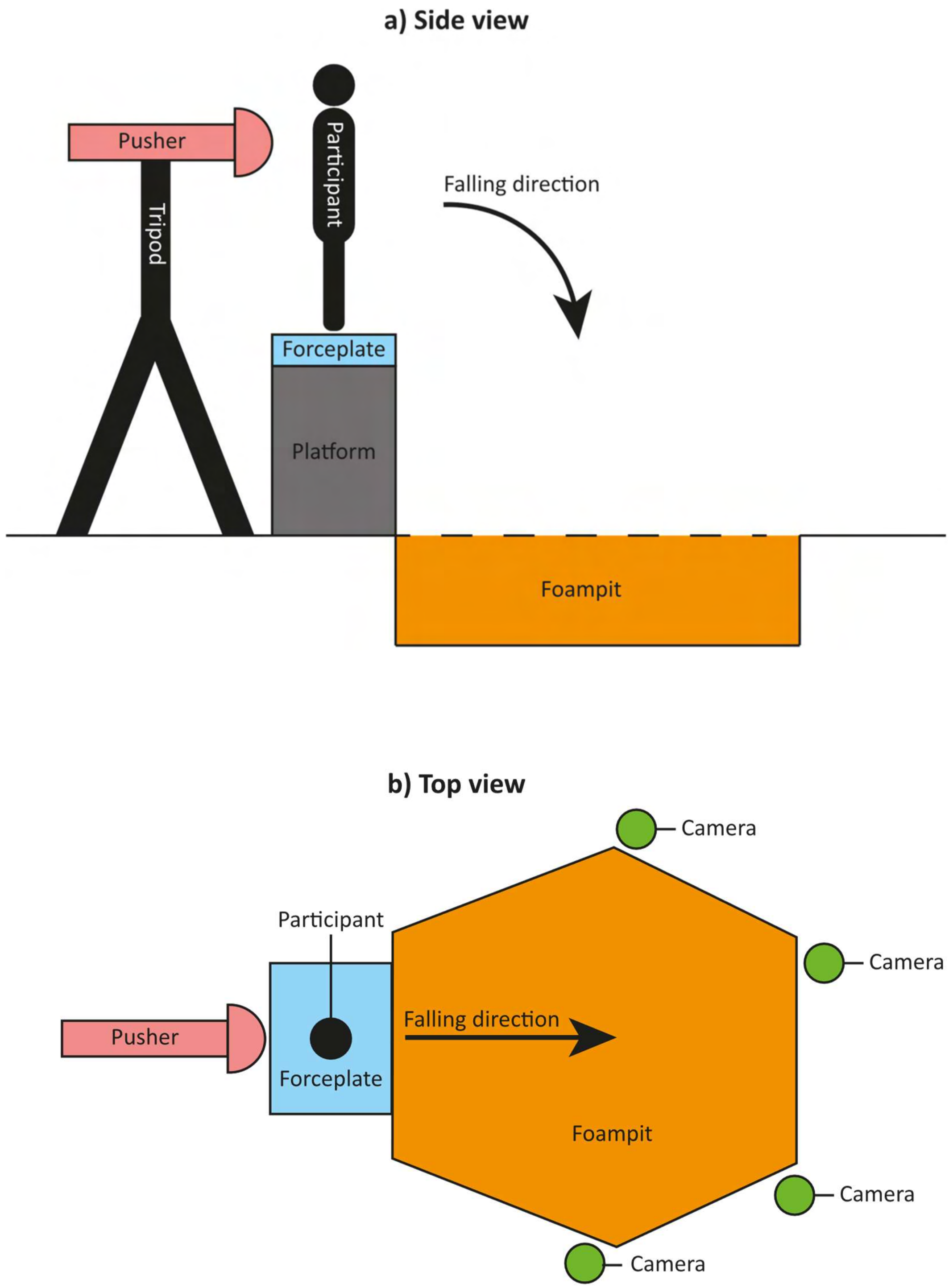


Figure 16 – An overview of the set-up used during the falling experiments, from a) a side view and b) a top view. The foampit was a recess in the floor filled with soft foam blocks. Next to the pit was the platform, 1.5 m higher than the pit. On top of the platform was the forceplate, a device that records the ground reaction forces of the participant standing on top of it. The pusher is placed behind the platform, and used to pushed the participant into the pit during a subset of trials. Four cameras are placed around the pit.

# Appendix C. Synchronisation

## C.1. Experiment Synchronisation

The four separate data-streams recorded during the experiment (forceplate, Xsens, cameras and, where applicable, pusher), needed to be synchronised before they could be processed further.

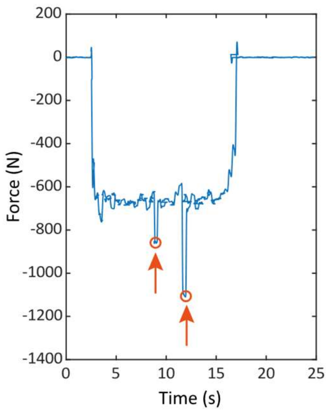


Figure 17 – The vertical ground reaction force from a typical passive fall. The arrows indicate the force peaks used to synchronise the forceplate with the cameras.

Figure 17 shows the vertical component of the ground reaction force for a typical passive fall, the force peaks caused by the participant's stomps on the plate are indicated with arrows. In both the Xsens kinematic data and the camera-footage, these stomps were marked manually. In the pushed falls, the pusher signal was synchronised to the forceplate through two additional force peaks. Figure 19 shows an example of the pusher force signal and vertical component of the ground reaction force for a typical pushed fall, the arrows indicate the force peaks produced for the synchronisation.

## C.2. Model Synchronisation

The simulation outcomes were synchronised with the experimental outcomes based on the ground reaction force of the participant and Madymo dummy, respectively, on the take-off platform. The vertical component of the ground reaction forces of a typical simulation, with the corresponding signal from the experiment, are plotted in Figure 18 with the arrow indicating the drop-off time-instance. The outcome measures were determined 0.3 s after this time-instance.

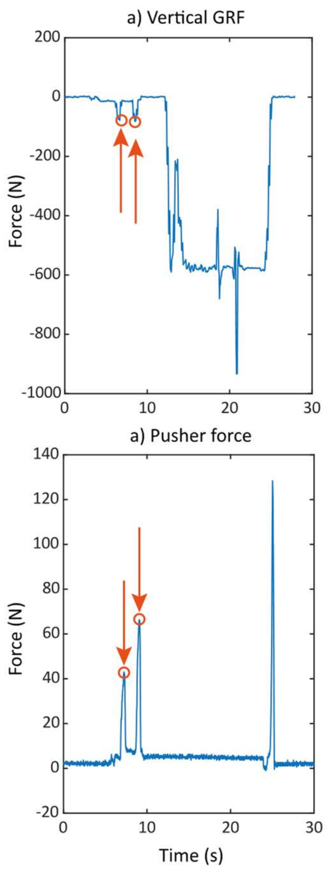


Figure 19 – The vertical component of the ground reaction force (a) and the push force (b) from a typical pushed fall. The arrows indicate the force peaks used to synchronise the forceplate with the pusher.

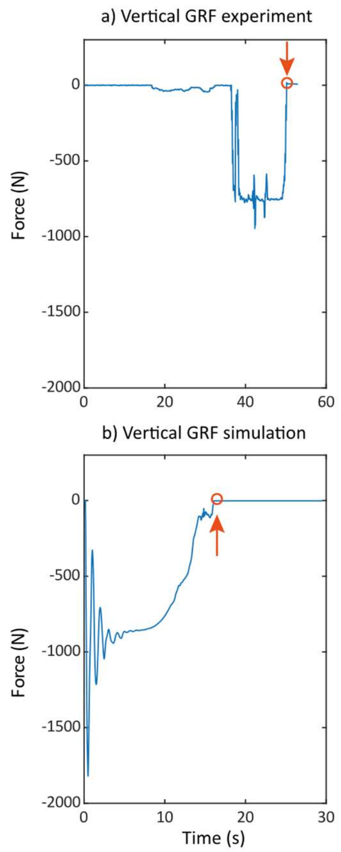


Figure 18 – The vertical ground reaction force from the experiment (a) and simulation (b) of a typical pushed fall. The arrows indicate the force peaks used to synchronise the simulation with the experiment.

## Appendix D. Experimental Trials

Table I – Overview of the order of falling conditions per participant used during the experiment. Participant 1 was part of a pilot measurement and is not included anywhere. The order was determined using a Latin square for participants 2-8, and randomised for 9 and 10. Participants 2 and 8 were not included in further analysis due to technical difficulties resulting in missing PiCam (video) data. The falling conditions referred to are passive backwards (PaBa), passive sideways (PaSi), pushed backwards (PuSi), pushed sideways (PuSi), jumped forward (JuFo) and stepped forward (StFo).

| Participant number | Trial 1-3 | Trial 4-6 | Trial 7-9 | Trial 10-12 | Note |
|---:|---:|---:|---:|---:|---:|
| 1 | - | - | - | - | Pilot |
| 2 | PaBa | PuSi | PaSi | JuFo | Not included in analysis: PiCam data missing |
| 3 | PuSi | JuFo | PaBa | PuBa | - |
| 4 | JuFo | PuBa | PuSi | StFo | - |
| 5 | PuBa | StFo | JuFo | PaSi | - |
| 6 | StFo | PaSi | PuBa | PaBa | - |
| 7 | PuBa | PaSi | PaBa | StFo | - |
| 8 | JuFo | PuSi | PaBa | PaSi | Not included in analysis: PiCam data missing |
| 9 | PaSi | PaBa | StFo | PuSi | - |
| 10 | PaBa | JuFo | PaSi | PuBa | - |

## Appendix E. Overview of Experiment to Model Joint Conversion

Table II – The conversion of joint types from Xsens kinematic output data to inputs accepted by Madymo. Refer to the Xsens user manual1 and the Madymo human body model manual2 for detailed information on the joints, joint types and degrees of freedom.

| Xsens | | | Madymo | | | | | | |
|---|---|---|---|---|---|---|---|---|---|
| | | | | Degrees of freedom | | | | | |
| **Joint description** | **Segment names** | **Segment number** | **Joint identifier** | **D1/R1** | **D2/R2** | **D3/R3** | **Joint type** | **Rotation order** | **Accepted input** |
| Complete human orientation | - | 1; 2 | Human_jnt | X / Roll right | Y / Pitch down | Z / Yaw left | - | - | R1-3 |
| Lower lumbar | L5-L3 and Pelvis-L5 | 2; 3 | LumbarLow-LumbarUp_jnt | Yaw right | Pitch down | Roll right | SPHE | - | Q1-4 |
| Upper lumbar | L3-T12 | 3; 4 | LumbarUp-TorsoUp_jnt | Roll right | Pitch down | Yaw left | FREE | - | Q1-4 |
| T1 | T8-Neck | 5; 6 | TorsoUp-NeckLow_jnt | Pitch down | - | - | REVO | Y | R1 |
| Neck joint | - | N/A | NeckLow-NeckUp_jnt | Roll right | Pitch down | Yaw left | - | - | - |
| Head OC | Neck-Head | 6; 7 | NeckUp-Head_jnt | Roll right | Pitch down | Yaw left | FREE | - | Q1-4 |
| Hips | Pelvis-RightUpperLeg | 1; 16 | HipR_jn | Roll right | Pitch down | Yaw left | SPHE | - | Q1-4 |
| | Pelvis-LeftUpperLeg | 1; 20 | HipL_jn | | | | | | |
| Knees | RightUpperLeg-RightLowerLeg | 16; 17 | KneeR_jnt | Pitch down | Roll left | Yaw left | FREE | - | Q1-4 |
| | LeftUpperLeg-LeftLowerLeg | 20; 21 | KneeL_jnt | | | | | | |
| Ankles | RightLowerLeg-RightFoot | 17; 18 | AnkleR_jnt | Yaw left | Roll right | Pitch down | SPHE | - | Q1-4 |
| | LeftLowerLeg-LeftFoot | 21; 22 | AnkleL_jnt | | | | | | |
| Shoulders | T8-RightUpperArm | 5; 9 | ShoulderR_jnt | Pitch down | Roll right | - | UNIV | YX | R1-2 |
| | T8-LeftUpperArm | 5; 13 | ShoulderL_jnt | | | | | | |
| Elbows | RigthUpperArm-RightForeArm | 9; 10 | ElbowR_jnt | Yaw left | Pitch down | - | UNIV | ZY | R1-2 |
| | LeftUpperArm-LeftForeArm | 13; 14 | ElbowL_jnt | | | | | | |
| Wrists | RightForeArm-RightHand | 10; 11 | WristR_jnt | Yaw left | Roll right | - | UNIV | ZX | R1-2 |
| | LeftForeArm-LeftHand | 14; 15 | WristL_jn | | | | | | |

[1] *MVN User Manual (2007-2009)*

[2] *Simcenter Madymo Human Body Models Manual (2020.2)*

## Appendix F. Statistical Results

All test statistics are from related-samples Wilcoxon signed-rank tests. The null hypothesis (H0) is that the median of differences between the two conditions equals 0. Significance level was α=.050.

### F.1. Experiment

Table III – Results of Wilcoxon signed-rank test comparing the backwards to the sideways falls from the experiment for each outcome measure.

| | | Median | | | | |
|---|---|---|---|---|---|---|
| **Outcome measure** | **N** | **Backwards** | **Sideways** | **Z** | **p** | **Decision** |
| Whole-body rotation | 14 | 10.0° | 87.4° | 3.296 | .001 | Reject H0 |
| Ledge angle | 14 | 3.7° | -8.9° | -2.856 | .004 | Reject H0 |
| Vertical angle | 14 | 48.0° | 59.0° | -0.310 | .975 | Retain H0 |

Table IV – Results of Wilcoxon signed-rank test comparing the passive to the pushed falls from the experiment for each outcome measure.

| | | Median | | | | |
|---|---|---|---|---|---|---|
| **Outcome measure** | **N** | **Passive** | **Pushed** | **Z** | **p** | **Decision** |
| Whole-body rotation | 14 | 28.1° | 45.4° | 1.977 | .048 | Reject H0 |
| Ledge angle | 14 | 0.0° | 0.8° | .910 | .363 | Retain H0 |
| Vertical angle | 14 | 59.0° | 47.0° | -.596 | .551 | Retain H0 |

### F.2. Simulations

Table V – Results of Wilcoxon signed-rank test comparing the backwards to the sideways falls from the simulations for each outcome measure.

| | | Median | | | | |
|---|---|---|---|---|---|---|
| **Outcome measure** | **N** | **Backwards** | **Sideways** | **Z** | **p** | **Decision** |
| Whole-body rotation | | | | | | |
| *Pushed Neutral* | | 0.0° | 17.4° | -1.859 | .063 | Retain H0 |
| *Pushed Extracted* | | -34.3° | 56.5° | -1.859 | .063 | Retain H0 |
| *Passive Neutral T1* | | -18.3° | 20.1° | -2.028 | .043 | Reject H0 |
| *Passive Neutral T2* | | -3.9° | 19.5° | -2.197 | .028 | Reject H0 |
| *Passive Neutral T3* | | -2.4° | 51.4° | -2.367 | .018 | Reject H0 |
| *Passive Neutral T4* | | 27.1° | 152.1° | -2.367 | .018 | Reject H0 |
| *Passive Extracted T1* | | -1.0° | 88.3° | -2.367 | .018 | Reject H0 |
| *Passive Extracted T2* | | 0.4° | 87.4° | -2.367 | .018 | Reject H0 |
| *Passive Extracted T3* | | 7.0° | 30.6° | -0.169 | .87 | Retain H0 |
| *Passive Extracted T4* | | 86.8° | 55.2° | 2.028 | .043 | Reject H0 |
| Ledge angle | | | | | | |
| *Pushed Neutral* | | 0.0° | -34.8° | 2.366 | <.001 | Reject H0 |
| *Pushed Extracted* | | 13.7° | -32.0° | 2.028 | .018 | Reject H0 |
| *Passive Neutral T1* | | -3.2° | -34.4° | 2.366 | .018 | Reject H0 |
| *Passive Neutral T2* | | -3.3° | -34.4° | 1.859 | .063 | Retain H0 |
| *Passive Neutral T3* | | -9.8° | -15.6° | .169 | .87 | Retain H0 |
| *Passive Neutral T4* | | -15.8° | 12.5° | -2.366 | .018 | Reject H0 |
| *Passive Extracted T1* | | -0.2° | -38.6° | 2.366 | .018 | Reject H0 |
| *Passive Extracted T2* | | -0.7° | -38.5° | 2.366 | .018 | Reject H0 |
| *Passive Extracted T3* | | 12.4° | -29.0° | 2.366 | .018 | Reject H0 |
| *Passive Extracted T4* | | 30.1° | 6.7° | 2.366 | .018 | Reject H0 |
| Vertical angle | | | | | | |
| *Pushed Neutral* | | 147.7° | 136.2° | 1.690 | .091 | Retain H0 |
| *Pushed Extracted* | | 142.3° | 124.3° | 2.366 | .018 | Reject H0 |
| *Passive Neutral T1* | | 163.8° | 134.4° | .0280 | .018 | Reject H0 |
| *Passive Neutral T2* | | 151.0° | 131.0° | 2.197 | .028 | Reject H0 |
| *Passive Neutral T3* | | 152.5° | 128.3° | 2.366 | .018 | Reject H0 |
| *Passive Neutral T4* | | 121.6° | 123.3° | -1.014 | .31 | Retain H0 |
| *Passive Extracted T1* | | 141.2° | 141.3° | 1.014 | .31 | Retain H0 |
| *Passive Extracted T2* | | 142.2° | 141.3° | .507 | .61 | Retain H0 |
| *Passive Extracted T3* | | 142.2° | 138.6° | 1.183 | .23 | Retain H0 |
| *Passive Extracted T4* | | 139.0° | 126.7° | 2.366 | .018 | Reject H0 |

### F.3. Comparison

Table VI – Results of Wilcoxon signed-rank test comparing the experiment to each of the simulation setups for each outcome measure.

| | | Median | | | | |
|---|---|---|---|---|---|---|
| **Outcome measure** | **N** | **Experiment** | **Simulation** | **Z** | **p** | **Decision** |
| Whole-body rotation | 14 | | | | | |
| *Pushed Neutral* | | 45.4° | 0.6° | 2.919 | .0035 | Reject H0 |
| *Pushed Extracted* | | | 41.4° | 1.915 | .056 | Retain H0 |
| *Passive Neutral T1* | | 28.1° | 6.2° | 2.291 | .022 | Reject H0 |
| *Passive Neutral T2* | | | 12.5° | 2.166 | .030 | Reject H0 |
| *Passive Neutral T3* | | | 35.4° | -.220 | .83 | Retain H0 |
| *Passive Neutral T4* | | | 41.0° | -2.668 | .0076 | Reject H0 |
| *Passive Extracted T1* | | | 42.0° | -.283 | .78 | Retain H0 |
| *Passive Extracted T2* | | | 42.9° | -.471 | .64 | Retain H0 |
| *Passive Extracted T3* | | | 29.6° | .848 | .40 | Retain H0 |
| *Passive Extracted T4* | | | 59.1° | -1.538 | .12 | Retain H0 |
| | | | | | | |
| Ledge angle | 14 | | | | | |
| *Pushed Neutral* | | 47.0° | -13.0° | 3.233 | .0012 | Reject H0 |
| *Pushed Extracted* | | | 9.0° | .0314 | .97 | Retain H0 |
| *Passive Neutral T1* | | 59.0° | -16.7° | 3.296 | <0.001 | Reject H0 |
| *Passive Neutral T2* | | | -25.2° | 2.982 | .0029 | Reject H0 |
| *Passive Neutral T3* | | | -12.7° | .659 | .51 | Retain H0 |
| *Passive Neutral T4* | | | 2.4° | -0.534 | .59 | Retain H0 |
| *Passive Extracted T1* | | | -19.3° | 2.982 | .0028 | Reject H0 |
| *Passive Extracted T2* | | | -17.5° | 2.417 | .016 | Reject H0 |
| *Passive Extracted T3* | | | -1.6° | -0.157 | .88 | Reject H0 |
| *Passive Extracted T4* | | | 12.9° | -2.856 | .0042 | Retain H0 |
| | | | | | | |
| Vertical angle | 14 | | | | | |
| *Pushed Neutral* | | 0.8° | 139.8° | -3.296 | <0.001 | Reject H0 |
| *Pushed Extracted* | | | 133.5° | -3.296 | <0.001 | Reject H0 |
| *Passive Neutral T1* | | 0.0° | 151.1° | -3.296 | <0.001 | Reject H0 |
| *Passive Neutral T2* | | | 143.6° | -3.233 | <0.001 | Reject H0 |
| *Passive Neutral T3* | | | 139.7° | -3.233 | <0.001 | Reject H0 |
| *Passive Neutral T4* | | | 122.5° | -3.296 | <0.001 | Reject H0 |
| *Passive Extracted T1* | | | 141.3° | -3.296 | <0.001 | Reject H0 |
| *Passive Extracted T2* | | | 141.4° | -3.296 | <0.001 | Reject H0 |
| *Passive Extracted T3* | | | 141.2° | -3.296 | <0.001 | Reject H0 |
| *Passive Extracted T4* | | | 130.3° | -3.296 | <0.001 | Reject H0 |